J. of Supercritical Fluids 56 (2011) 33–40

Contents lists available at ScienceDirect

The Journal of Supercritical Fluids

journal homepage: www.elsevier.com/locate/supflu

Estimation of lower flammability limits in high-pressure systems. Application to the direct synthesis of hydrogen peroxide using supercritical and near-critical CO_2 and air as diluents

C.M. Piqueras [a], J. García-Serna [b,*], M.J. Cocero [b]

[a] Planta Piloto de Ingeniería Química, Universidad Nacional del Sur, CONICET, CC 717, 8000 - Bahía Blanca, Argentina
[b] High Pressure Process Group, Chemical Engineering & Environmental Technology Department, University of Valladolid, Prado de la Magdalena sn, 47011 - Valladolid, Spain

ARTICLE INFO

Article history:
Received 12 July 2010
Received in revised form
18 November 2010
Accepted 18 November 2010

Keywords:
Lower flammability limit
Hydrogen peroxide
Direct synthesis
Supercritical carbon dioxide
High pressure

ABSTRACT

A method for the prediction of the LFL at high pressures, where data are scarce, based on the calculation of adiabatic flame temperatures for the mixtures $H_2 + O_2$ in CO_2 and N_2, between 1.0 and 300 bar and 288–348 K is presented. A group contribution equation of state (GC-EoS) has been selected to predict thermodynamic properties of the mixture, i.e. residual enthalpy, heat capacity and others, as well as phase equilibrium data, giving deviations lower than 10% at high pressures. The use of CO_2 as a diluent increases the operational margin from 4.5 mol% H_2 at 1 bar up to ca. 7.0–9.0 mol% H_2 at 200 bar due to the increase in the heat capacity. On the other hand, the use of nitrogen or air as a diluent only increases the margin from 5.2 mol% H_2 at 1 bar up to ca. 6.0 mol% H_2 at 200 bar.

1. Introduction

The operation at high pressures modifies the flammability limits and, many estimation methods as well as experimental data are, respectively, prepared or measured for pure substances either in air or other diluents in combination, usually at atmospheric conditions [1].

The estimation of flammability limits has been carried out using different methods, i.e. empirical correlations [2], group contributions methods [3], net heat of combustion methods [4,5], analytical methods [6,7], kinetic theory studies [8] and Gibbs free energy minimization [9]. For instance, Albahri [3] used the Joback definition of group contributions methods, modifying it to account for the location of the structural groups in the molecule to predict the flammability characteristics in pure hydrocarbons. Seaton [5] has derived a mathematical model from Le Chatelier's law in order to estimate flammable limits of vapors in air, using also a group contribution procedure. Hshieh [4] developed a method to predict the low flammability limit of organic and organo-silicon compounds from the net heats of combustion. Vidal et al. [6,7] has reported different methods based on chemical equilibrium, which is calculated by minimization of Gibbs free energy. Egolfopoulos et al. carried out the simulation of freely propagating flames with the inclusion of detailed descriptions of chemical kinetics and molecular transport, in order to determine lean flammability limits of CH_4/air and C_3H_8/air mixtures [8]. Shebeko et al. [9] proposed an analytical method for the calculation of flammability limits in mixtures of combustible-oxidizer-diluents based on the calculation of adiabatic flame temperatures. Their results show an acceptable accuracy for practical applications at low pressures, obtaining mean square deviations for the lower flammability limit of 12.6% (with 195 points) and 11.3% (74 points), respectively, for chemically inert and halogenated agents. Finally, Melhem [10] proposes a method minimizing Gibbs free energy obtained from a Peng–Robinson equation of state, using a modified mixing rule equations, in order to predict the global equilibrium.

For the case of the direct synthesis of H_2O_2, considered in this paper, explosion hazards associated to H_2 are an extremely important issue and operation under flammability limits is indispensable [11]. The process is carried out in a three-phase reactor: solid–liquid–gas, either trickled bed or slurry bubble column reactor. In order to increase mass transfer between the gas and liquid phases, the system is pressurized between 30 and 120 bar as an average interval [12]. The use of CO_2 as a reaction medium for producing H_2O_2 in situ by reacting H_2 and O_2 was previously proposed [13]. Diluting the gas phase ($H_2 + O_2$) using CO_2 is an alternative that, according to Pande and Tonheim [14], increases the lower flammability limit (LFL) of H_2/air mixtures up to 9.5% for H_2 at

* Corresponding author. Tel.: +34 983184934; fax: +34 983423013.
E-mail addresses: jgserna@iq.uva.es, jgserna@gmail.com (J. García-Serna).

0896-8446/$ – see front matter © 2010 Elsevier B.V. All rights reserved.
doi:10.1016/j.supflu.2010.11.013

Nomenclature

A	Helmholtz's energy
c	speed of sound ($m\,s^{-1}$)
Cp	heat capacity of real gases mixture ($J\,mol^{-1}\,K^{-1}$)
$Cp^{IG}{}_m$	heat capacity of ideal gases mixture ($J\,mol^{-1}\,K^{-1}$)
d_c	value of the hard sphere diameter at the critical temperature for the pure component (m)
d_j	hard-sphere diameter for 1 mol of species j (m)
G^r	residual Gibbs energy of the mixture (J)
g_{ij}	attraction energy parameter for interactions between groups i and j
$g^*{}_{jj}$	interaction parameters for reference temperature $T^*{}_i$
$g^*{}_{jj}$	GCA-EoS pure-group parameters
$g''{}_{jj}$	GCA-EoS pure-group parameters
k	surface fraction of group k, k_{ij} = GC-EoS binary interaction parameters
$k^*{}_{ij}$	interaction parameters for reference temperature $T^*{}_i$
$k^*{}_{ij}$	GC-EoS binary interaction parameters
$\Delta\mathcal{H}_{Reac}$	energy released by the reaction at the inlet temperature and pressure
$\Delta\mathcal{H}_R$	enthalpy of the reactants, integrated from initial pressure and temperature to 298 K, 1 bar
$\Delta\mathcal{H}_{Ad}$	adiabatic enthalpy variation from reference temperature to the final temperature at constant pressure
$\Delta\mathcal{H}^{id}$	ideal gas enthalpy variation from reference temperature to the final temperature at constant pressure
LFL	low flammability limit
n	number of moles
NC	number of components
NG	number of groups
P	pressure (Pa)
R	universal gas constant
$\tilde{q}$	total number of surface segments
q_j	number of surface segments assigned to group j
T	temperature (K)
$T^*{}_i$	reference temperature (K)
MW	molecular weight ($kg\,kg\,mol^{-1}$)
V	total volume (m^3)
v_{ji}	number of groups type j in molecule i
z	number of nearest neighbours to any segment (always set to 10)

Greek letters

α_{ij}	is the non-randomness parameter (adjustable)
φ_i	fugacity coefficient of each component
att	attractive term

Subindex

att	attractive term
c	critical
exp	experimental data
calc	calculated using a model or equation
i	component

Superindex

fv	free volume

atmospheric pressure. A significant advantage of using $scCO_2$ is the ability to exploit its pressure-tunable heat capacity, which exhibits a maximum in the near-critical region. This unusually high heat capacity of CO_2 in the near-critical region can be used to effectively absorb the heat generated from H_2 oxidation reactions, in order to achieve greater H_2 concentrations and a better temperature control [14–16].

The aim of this work is to develop an strategy to estimate H_2 concentration limits, allowing for the safe operation in the direct synthesis of hydrogen peroxide at high pressures. The predictions have been made for both CO_2 and N_2 as diluents, bearing in mind that air is more economic as an oxidant than pure O_2 at industrial scale. Because of the impossibility of a direct calculation via group contribution methods for H_2/O_2 + diluent mixtures, we present an adaptation to high-pressure conditions of the procedure proposed by Shebeko et al. [9]; the proposed method estimates the adiabatic flame temperature of a gas mixture under equilibrium conditions for combustion using an specific EoS for modeling high-pressure phase behavior.

2. Modeling

2.1. LFL prediction method

The flammability limit is associated with a certain generation rate of critical energy as well as with a certain level of temperature in which the reactions occurring in the flame are stable. According to Shebeko et al. [9], the critical reaction temperature at the LFL composition can be assumed to be equivalent to the adiabatic flame temperature, because the process is supposed to be adiabatic. This statement is based on the assumption that during the deflagration, heat losses in the flame front, in direction of the propagation, are several orders of magnitude higher than heat losses in the boundary walls. It is commonly considered that all the free-radical reactions occurring in the flame front can be summarized as a single main reaction describing the bulk process. Assuming these conditions, the adiabatic flame temperature (AFT) indicates the maximum temperature of the process that avoids flame propagation. The calculation of AFT in a batch reactor during H_2 combustion with O_2 using CO_2 and air as diluents can be made by solving the mass and energy balances [9]. Temperature and pressure range were 298–348 K and 1.0–150 bar respectively; the same range used in the H_2O_2 direct synthesis [17,18]. In some cases, calculations up to 300 bar were made to analyze the results at extreme conditions. At a fixed reaction pressure and composition, AFT was computed assuming that: (a) the reaction occurs at uniform temperature and pressure, (b) the reagents are in a single phase and the feed ratio between H_2 and O_2 is kept constant, (c) the product mixture is maintained in vapor phase at 298 K, 1 bar, (d) H_2 and O_2 are assumed to react instantaneously and completely, (e) the heat of reaction is −241 kJ per mole of hydrogen consumed [9], (f) nitrogen is assumed to be an inert when used as diluent (i.e. no nitrogen oxides formation) in the range of temperatures and pressures studied. Based on these assumptions the energy balance is given by Eq. (1).

$$\Delta\mathcal{H}_{Reac}(298\,K, 1\,bar, n) = \Delta\mathcal{H}_R(T_{in}, P, n) + \Delta\mathcal{H}_{Ad}(AFT, P, n) \quad (1)$$

where $\Delta\mathcal{H}_{Reac}$ is the energy released by the reaction at the inlet temperature and pressure, $\Delta\mathcal{H}_R$ is the reactants enthalpy, integrated from initial pressure and temperature to 298 K, 1 bar, $\Delta\mathcal{H}_{Ad}$ is the adiabatic enthalpy from reference temperature to the final temperature at constant pressure.

The enthalpies for all the components involved were calculated as the sum of ideal and residual contributions (Eq. (2)). The residual contribution in the mixture is related to the EoS as described in Eq. (3), where $\hat{\varphi}_i$ is the fugacity coefficient of each component in the mixture, and R is the constant of gases.

$$\Delta\mathcal{H} = \Delta\mathcal{H}^{ig} + \Delta\mathcal{H}^{R} \quad (2)$$

$$\Delta \mathcal{H}^R = -RT^2 \sum_i^{NC} \left(\frac{\partial \ln \hat{\varphi}_i}{\partial T} \right)_{P,n} \quad (3)$$

The AFT was estimated following the steps indicated below:
Procedure 1:

a. Pressure, initial temperature and O_2/H_2 ratio are fixed.
b. $\Delta \mathcal{H}_{Reac}$, is obtained from the literature accounting the H_2 vol%, $\Delta \mathcal{H}_R$, is determined directly from Eqs. (2) and (3).
c. An initial adiabatic temperature guess (seed value) is assumed, $\Delta \mathcal{H}^R$ is calculated integrating Cp value from inlet temperature to the actual adiabatic temperature. Then $\Delta \mathcal{H}^R$ is obtained at the final temperature and pressure. Through the Newton–Raphson method, AFT is found when its value makes that $\Delta \mathcal{H}_{Ad}$ complete the energy balance.

As suggested by other authors [9], LFL is calculated by means of an inverse procedure, as explained next:
Procedure 2:

a. Fix a threshold temperature (a "critical" reaction temperature), which is associated to the necessary energy to overcome the limit for free radical formation [8].
b. Propose a H_2 vol% as initial guess (seed).
c. By means the Newton–Raphson method, AFT is calculated (*Procedure 1*) in a inner loop. After this, the obtained AFT value is compared against the threshold temperature.
d. The Newton–Raphson method varies H_2 vol% and until the AFT equals the threshold temperature within ±0.5 K. In this point H_2 vol% is the searched LFL.

For our case study the threshold temperature was estimated assuming the combustion of H_2 in air at 298 K and 1 bar, as described in the next section.

2.2. Thermodynamic model

GC-EoS model is a group contribution equation of state, proposed by Skjold-Jørgensen [19,20] designed to predict solubility of gases in vapor–liquid equilibrium (VLE). This model is presented in the residual Helmholtz function plane with their natural variables $(T, V, \mathbf{n})$, being V the total volume and $\mathbf{n}$ the vector of molar composition. The model is based on two contributions to the residual Helmholtz function: repulsive or free volume and attractive part. The free volume contribution is modeled by assuming a hard sphere behavior for the molecules, characterizing each substance i by a hard sphere diameter d_i. The model adopt a Carnahan–Starling [21] type of hard sphere expression for mixtures (Eq. (4))

$$\left(\frac{A}{RT}\right)^{fv} = 3\left(\frac{\lambda_1\lambda_2}{\lambda_3}\right)(Y-1) + \left(\frac{{\lambda_2}^3}{{\lambda_3}^2}\right)(-Y + Y^2 - \ln Y) + n \cdot \ln Y \quad (4)$$

with

$$Y = \left(1 - \frac{\pi\lambda_3}{6V}\right)^{-1} \quad (5)$$

$$\lambda_k = \sum_i^{NC} n_j d_j^k \quad (6)$$

where n_j is the number of moles of component j, NC stands for the number of components, V represents the total volume, d_j the hard-sphere diameter for 1 mol of species j, R stands for universal gas constant. In this case, the original expression for the hard sphere diameter proposed by Skjold-Jørgensen [19,20] was utilized for the hard-sphere critical diameter determination based on the critical properties of the pure component (T_c, P_c) [22], Eq. (7). The expression for the temperature dependence of the hard sphere diameter d_i, assumed as described by Eq. (8).

$$d_c = \left(0.08943 \cdot \frac{RT_c}{P_c}\right)^{1/3} \quad (7)$$

$$d_i = 1.065655 \cdot d_c \left[1 - 0.12 \cdot \exp\left(\frac{-2T_c}{3T}\right)\right] \quad (8)$$

where d_c is the value of the hard sphere diameter at the critical temperature, T_c, for the pure component. For the evaluation of the attractive contribution to the Helmholtz energy, a group contribution version of a density dependent NRTL-type expression [23] is derived, Eq. (9)

$$\left(\frac{A}{RT}\right)^{att} = -\frac{z}{2} \frac{\sum_i^{NC} n_i \sum_j^{NG} v_j^i q_j \sum_i^{NC} (\theta_k g_{kj} \tilde{q} \rho)}{\sum_i^{NC} \theta_l \tau_{ij}} \quad (9)$$

With,

$$\theta_j = \left(\frac{q_j}{q}\right) \sum_i^{NC} n_i v_j^i \quad (10)$$

$$q = \sum_i^{NC} n_i \sum_i^{NG} v_j^i q_j \quad (11)$$

$$\tau_{ij} = \exp\left[\frac{\alpha_{ij} \Delta g_{ij} \tilde{q}}{RTV}\right] \quad (12)$$

$$\Delta g_{ij} = g_{ij} - g_{jj} \quad (13)$$

where z is the number of nearest neighbours to any segment (always set to 10), NG represents number of groups, v_{ji} is the number of groups type j in molecule i, q_j stands for the number of surface segments assigned to group j, k represents the surface fraction of group k, $\tilde{q}$ is the total number of surface segments, α_{ij} is the non-randomness parameter (adjustable), g_{ij} stands for the attraction energy parameter for interactions between groups i and j, and ij is the NRTL [23] non-randomness parameter. The interactions between unlike groups are calculated from Eq. (14).

$$g_{ij} = k_{ij}(g_{ii}g_{jj})^{1/2} \quad (14)$$

with ($k_{ij} = k_{ji}$) and the temperature dependences for the interaction parameters are given in Eqs. (15) and (16).

$$g_{ij} = g_{jj}^* \left(1 + g'_{jj} \frac{T}{T_j^* - 1} + g''_{jj} \ln \frac{T}{T_j^*}\right) \quad (15)$$

$$k_{ij} = k_{ij}^* \left\{1 + k'_{ij} \ln \left[\frac{2T}{T_i^* + T_j^*}\right]\right\} \quad (16)$$

where g^*_{jj} and k^*_{ij} are the interaction parameters for reference temperature T^*i, g^*_{jj} and g''_{jj} represent the GCA-EoS pure-group parameters, k_{ij} and k^*_{ij} stand for the GC-EoS binary interaction parameters. This model has proven to be successful in predicting phase equilibrium of several binaries around the critical point [20] as well as more complex scenarios involving size-asymmetric [24] mixtures, in particular, vapor–liquid equilibrium (VLE), liquid–liquid equilibrium (LLE), where phase behaviors are adequately predicted with a single set of parameters.

Fig. 1 shows the predictions of the model against a set of experimental data for some of the binaries involved in the reaction of hydrogen peroxide production [25–27]. In this case, the original set of interaction parameters [19,20] was used obtaining predictions with deviations lower than 8% for the compositions of the liquid phase and 3% for the vapor phase up to 300 bar and 383 K

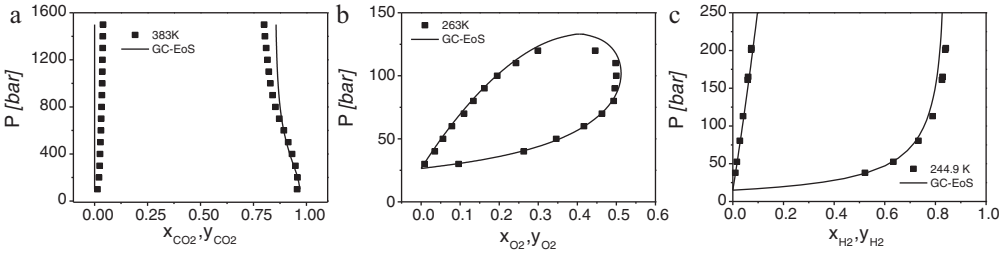

Fig. 1. Phase behavior prediction of GC-EoS equation of state of the components involved in the H_2O_2 direct synthesis. (a) Water–carbon dioxide [27], (b) oxygen–carbon dioxide [25], and (c) hydrogen–carbon dioxide [26].

for H_2O–CO_2 binary mixtures. In the case of O_2–CO_2 system, the deviations in the composition were lower than 3% for the liquid phase and 5% for the vapor phase at 263 K for 124 bar. Similarly, for $H_2 + CO_2$ mixtures the errors in the prediction of the composition were lower than 2% for the liquid phase and 8% for the vapor phase up to 203 bar at 244.9 K.

3. Results and discussion

3.1. Validation of the predicting LFL method

As it was mentioned before, the LFL is associated with a certain critical reaction temperature. We have estimated this threshold temperature from the LFL values reported in the literature for H_2 combustion at 1 bar using pure O_2. These values vary in the range of 4 vol% (AFT = 601 K) up to 4.5 vol% (AFT = 640 K). We have taken an average LFL of 4.25 vol% [28], being the calculated AFT equal to 620 K. The effect of this assumption is discussed later, comparing the results at different pressures.

Although the H_2 combustion is well known, scarce experimental measurements have been made at high pressure conditions. In order to evaluate the H_2 combustion at higher pressures the threshold temperature is assumed to be constant with pressure, i.e. the activation volume is neglected.

This assumption has been evaluated using two sets of data. First, one set of LFL data of H_2 combustion in air as well air in combination with N_2 and CO_2 as diluents [29]. In that research, the authors used a steam apparatus designed for determining flammability limits in the pressure range from 1 to 40 bar and the temperature range 293–523 K. It comprised a reaction vessel in the form of a vertical cylinder where the mixture was ignited by means of an incandescent wire. Second, a set of experimental data of H_2–air explosions carried out in a 2.7 L spherical bomb, which followed the European norm prEN 1839, at pressures between 1 and 200 bar [30].

Fig. 2 shows how experimental data for LFL exhibit an abrupt increase in the range between 1 and 10 bar. This behavior is not well predicted by the model proposed, which exhibits a flatter behavior. Nevertheless, at pressures higher than 20 bar the linear tendency shown by the prediction has a similar slope than experimental data. In order to improve the prediction at higher pressures, where the direct synthesis of H_2O_2 is favoured [17,18], a LFL of 5.3 vol% is assumed at 1 bar (equivalent to AFT of 720 K for mixtures with air as diluent). Table 1 shows the comparison between the experimental data and results of the simulation using this threshold temperature. The agreement is satisfactory considering the variation of the data found in this kind of experiments, where LFL values determined in closed vessels with upward propagation tend to be 20% lower than in other devices [7].

Fig. 2 also includes the results above mentioned at 288 K, 353 K and the LFL data for variations in the concentration of N_2. The experimental values are ca. 10% higher (Table 1) than the predicted values for the pressure range investigated variating N_2 concentration. The prediction is better at higher pressures, where the average deviation is 1.5% respect to the explosion data. The dashed line represents the predictions using the value of 4.25 H_2vol% at 1 bar.

3.2. Estimation of the adiabatic flame temperatures

Adiabatic flame temperature was estimated in the same range of temperature and pressure than the H_2O_2 direct synthesis is carried out [11,17,18]. This means, an inlet temperature (temperature before the H_2 combustion) from 288 to 348 K, from 1 to 150 bar and a H_2 volume percentage from 4 up to 7 vol%.

3.2.1. Pressure variation

Fig. 3(a) shows the results of the AFT estimation as a function of pressure, when the combustion takes place at inlet temperature of 288, 308 and to 348 K for a mixture with 7 vol% H_2 in CO_2, and a O_2/H_2 molar ratio of 2. At lower pressures, higher AFT values are obtained. At low initial temperature a sudden decrease of AFT is

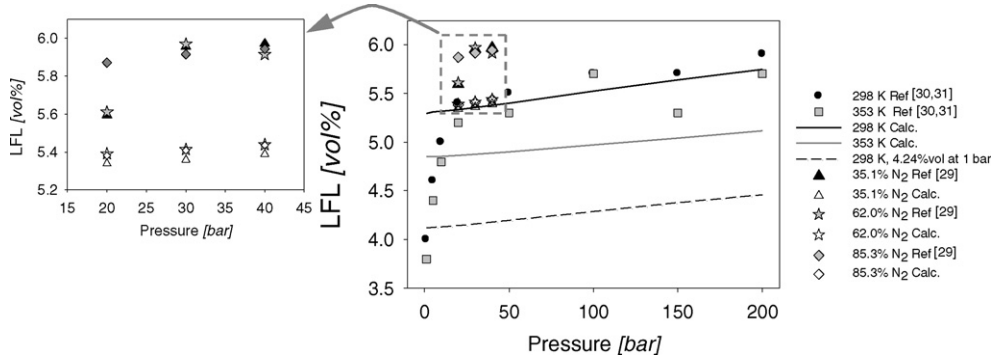

Fig. 2. Comparison between LFL calculated whit the algebraic method against to experimental values obtained from the literature. (a) Values obtained from Shebeko et al. [29] which uses air and extra N_2 is added to the mixture and values of H_2 explosion whit air from Refs. [33,34]. The measurements carried out following the bomb modified method following the draft of the new European standard for the determination of explosion limits (prEN 1839), bomb of 2.7 L.

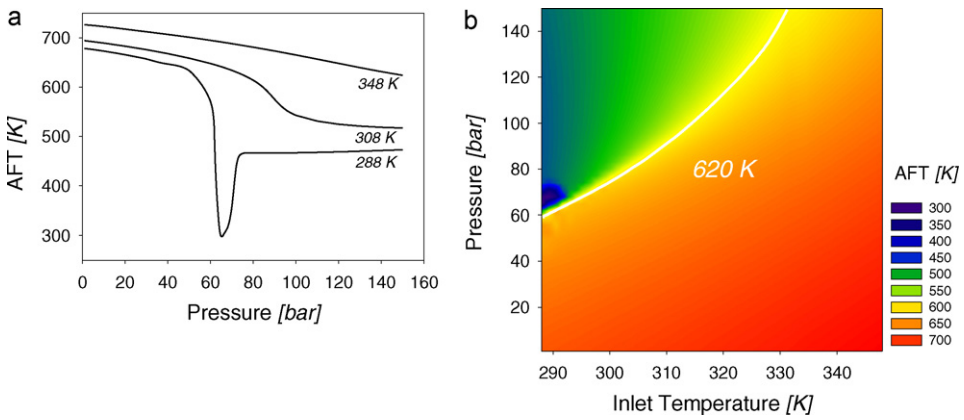

Fig. 3. Adiabatic flame temperature (AFT) of the mixture after the combustion of 7%vol $H_2 + O_2$ (O_2/H_2 molar ratio of 2) in CO_2. (a) AFT profile for a combustion at constant inlet temperature. (b) Contour plot of AFT as parameter in K, varying inlet temperature and pressure.

observed around of the CO_2 critical point (approximately 69 bar and 290 K for this composition).

3.2.2. Inlet temperature variation

Fig. 3(b) shows a contour plot of AFT values as parameter with inlet temperature and pressure as variables for the same mixture than Fig. 3(a). These results reveal that at low temperatures and pressures, the mixture has gas-like properties (lower heat capacities) and high AFT values are observed. The temperature rise produced a moderate increase of the AFT values which is explained by the higher energy available in the initial mixture. On the other hand, in a narrow range from 60 up to 73 bar, and from 286 to 294 K, AFT decreases rapidly, which represents more clearly the phenomena observed in Fig. 3(a).

These results are explained by the phase transition of the mixture through the critical point, which involves an abrupt increment of heat capacity (Cp) of the mixture. Phase changes around this point are gradual for the first derivatives of Gibbs energy such as enthalpy, molar volume and internal energy (ΔH, ΔV, and ΔU), but a indetermination of the specific heat (which is the second order derivative of Gibbs energy) occurs at this specific value.

Table 1
Validation of the prediction method. Experimental data for H_2 combustion in air in combination with air and added N_2 as diluent. A threshold temperature of 620 K was used for the estimation.

P [bar]	N_2 [vol%]	Exp. LFL [vol%]	Calc. LFL [vol%]	Deviation [%]
20*	89	5.87	5.38	8.54
	91	5.61	5.39	9.30
	92	5.60	5.34	9.99
30*	82	5.91	5.41	8.34
	86	5.97	5.41	3.92
	91	5.95	5.36	4.56
40*	83	5.94	5.44	8.52
	88	5.91	5.44	8.03
	92	5.97	5.39	9.73
1	79#	4.90	5.37	9.59
10	79#	4.95	5.39	8.89
100	79#	5.25	5.63	7.24
1	0&	4.00	5.30	24.5
5	0&	4.60	5.31	13.4
10	0&	5.00	5.32	6.0
20	0&	5.40	5.33	1.2
50	0&	5.50	5.40	1.9
100	0&	5.70	5.52	3.2
150	0&	5.70	5.64	1.1
200	0&	5.90	5.75	2.6

The N_2 percentage is global percentage of diluent in the mixture.
Deviation [%] $= \frac{|LFL_{Exp} - LFL_{Calc}|}{LFL_{Exp}} \times 100$.
* $H_2 + O_2 +$ air $+ N_2$ system [29].
# $H_2 + O_2 +$ air from Ref. [33].
& $H_2 + O_2$ from Ref. [34].

3.2.3. Heat capacity behavior

An increase of several orders of magnitude on Cp value occurs around the critical point. Then, in this region the drop in AFT determines a zone where the mixture in supercritical state presents great fluctuations of their properties. Above to 296 K, a decrease of the AFT values is observed due to the transition of the gas-like to liquid-like heat capacities. This transition decreases in intensity when pressure and inlet temperature are increased from 60 to 150 bar and 288 to 330 K. Above these conditions a monotonic decrease of AFT is observed.

Fig. 4 presents the values of heat capacity calculated for 7% H_2O + 7% O_2 + 86% CO_2 (vol%) mixture and for a inlet temperature of 288 K by means of Eqs. (17) and (18). It shows that the enlargement of Cp value in the critical point neighborhood is almost 2 orders of magnitude higher than the value of heat capacity in liquid phase. This increase is more pronounced around 70 bar, where the highest variations of AFT were found. Thus, when the combustion is carried out at thermodynamic conditions around the CO_2 critical point low values of AFT will be expected, and the mixture could take in certain

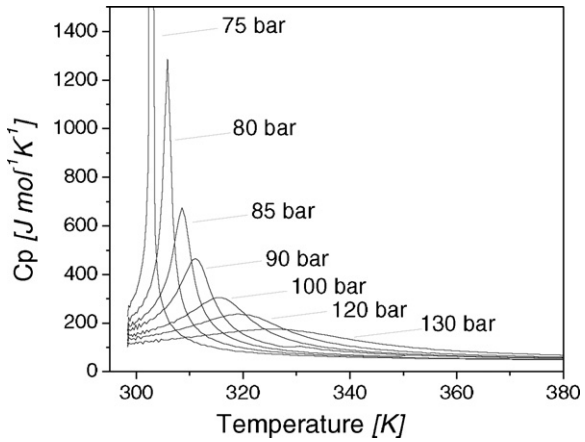

Fig. 4. Variation of mixture heat capacity 7% O_2 + 7% H_2O + 86% CO_2 (vol%) in the range of 298 K up to AFT at constant pressure as parameter.

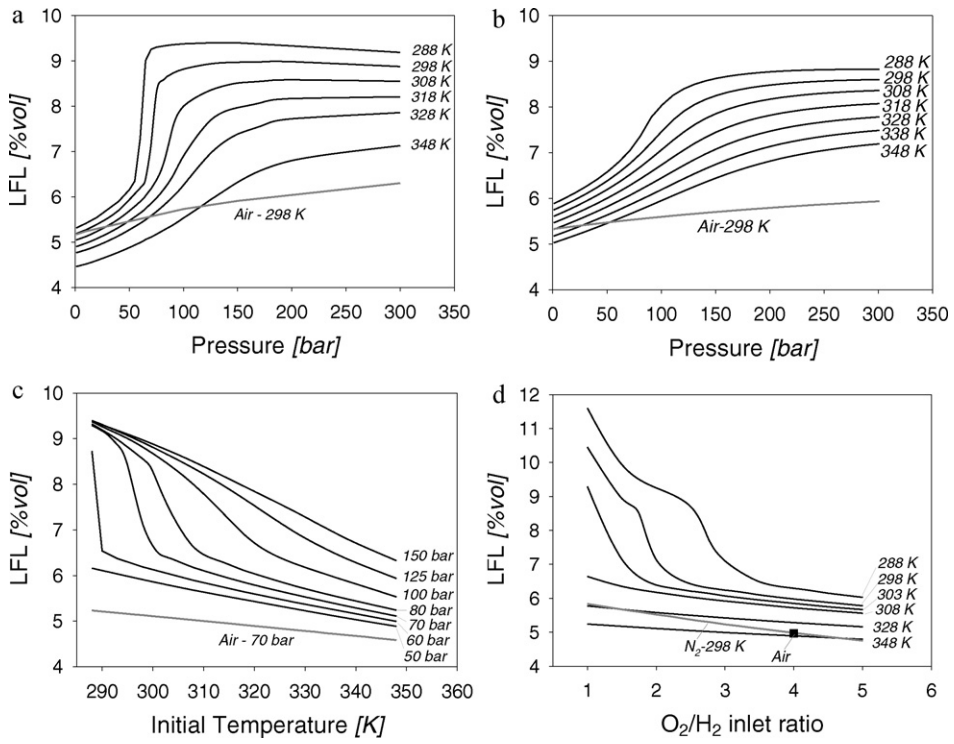

Fig. 5. Low flammability flame (LFL) values within the range of temperature and inlet temperature and pressure as parameter. (a) LFL variation with pressure at $O_2/H_2 = 2$ and inlet temperature as parameter, (b) LFL variation calculated using SKR-MHV2 equation of state by means of the commercial software ASPEN PLUS 7.0 for the same conditions than figure (a), (c) LFL variation whit inlet temperature at same feed ratio as figure (a) and pressure as parameter, and (d) LFL variation whit the O_2/H_2 feed ratio at 70 bar and inlet temperature as parameter.

amount of extra heat.

$$Cp = Cp_{mix}^{IG} + \left(\frac{\partial^2 G^r(T,P,\mathbf{n})}{\partial T^2}\right)_{P,n} \quad (17)$$

$$G^r(T,P,\mathbf{n}) = RT\sum_i n_i \ln \hat{\varphi}_i \quad (18)$$

Therefore, the advantage of using near-critical or supercritical CO_2 ($scCO_2$) in this case is based on its pressure-tunable heat capacity which allows for a major control of the temperature rise in the reactor carrying out exothermic reactions [31]. Outside this zone, up to 330 K a monotonic decrease takes place for all pressures in the range investigated.

The white line in Fig. 3(b) indicates the boundary in which the AFT is equal to the threshold temperature of 620 K for CO_2, which corresponds to 5.3 vol% of H_2 value fitted to the experimental data. Above this line can be considered as a safe operational zone.

3.3. Influence of diluents on the low flammability limit: CO_2 vs N_2

3.3.1. Pressure variation

Fig. 5(a) presents the results of the LFL determination with pressure variation for a $H_2 + O_2 + CO_2$ mixture using a $O_2/H_2 = 2$ (molar ratio). An abrupt increase of the LFL from 5.3 vol% to more than 9.0 vol% is found when the reaction takes place at pressures between 50 and 70 bar (near the critical point of CO_2) and at inlet temperatures below 313 K. So, the benefit is the increase of the combustible percentage in the reactants mixture and, in this particular reaction, possible H_2O_2 yield increase. This behavior is highly non-linear, similarly to the variations of the heat capacity observed in the transition through the critical point zone (0.9 up to 1.2 times of the critical pressure). The benefits of the Cp enlargement are reduced when the initial temperature is higher than the CO_2 critical temperature.

3.3.2. Commercial software: Aspen Plus

Fig. 5(b) presents the same calculation but made using the commercial software package Aspen Plus ONE7. A sensibility analysis of an adiabatic batch reactor was made using the property model Soave–Redlich–Kwong equation of state with MHV2 mixing rules [32], calculating the H_2 molar fraction in the out stream. As it can be seen from the figure the commercial software exhibits the same trend behavior than the results using GC-EoS. Deviations below 5% were obtained for pressures from 120 to 150 bar, while the predictions near the critical pressure (60–90 bar) are considerably different. These differences in the prediction of the LFL are caused by the differences in the prediction of the residual properties obtained by both models at lower temperatures in the critical region.

3.3.3. Inlet temperature variation

Fig. 5(c) shows the LFL values calculated for the same system than Fig. 5(a) (O_2/H_2 ratio of 2), when inlet (or initial) temperature is varied from 288 up to 348 K. Increasing this temperature, the system starts from a higher internal energy and so, the LFL decreases. The curves above 70 bar show an abrupt decrease at initial temperatures below 300–310 K. At higher pressures, from ca. 150 bar, the LFL decrease gradually following the same behavior than liquid heat capacity with temperature.

3.3.4. O_2/H_2 feed ratio

Similarly, LFL decreases when the composition of the products is changed raising the O_2/H_2 feed ratio from 1 to 5. This effect is presented in Fig. 5(d), which shows the values of LFL calculated for 70 bar and constants values of inlet temperature as parameter. The results are explained by a decrease of the heat capacity of the mixture, caused by the reduction of the CO_2 molar content. The major changes occur between O_2/H_2 of 1.5 and 3 for initial temperatures below 303 K, near the critical point of CO_2, similarly to the

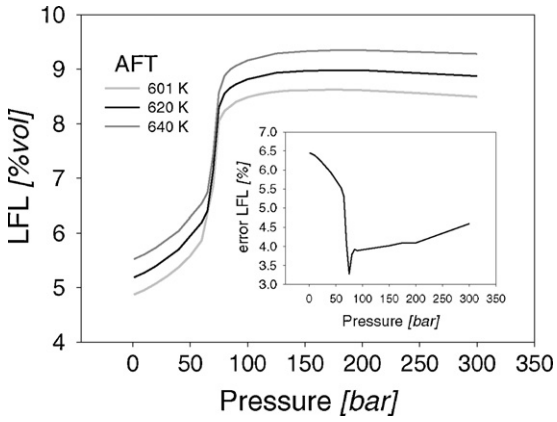

Fig. 6. LFL comparison for the values calculated for AFT values with pressure corresponding to 4 and 4.5 vol% of H_2 in CO_2 as diluent for initial temperature of 298 K. The detail shows the variation of the error percent of LFL predicted for 640K respects to the average value.

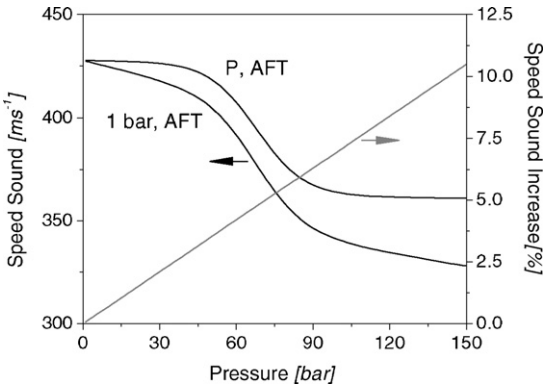

Fig. 7. Speed of sound for 7% O_2 + 7% H_2O + 86% CO_2 (vol%) mixture as starting temperature of 288 K and percentage ratio between the conditions of high-pressure and atmospheric pressure, both at the same AFT.

previous observations. These higher LFL values cause lower perturbations of the system in the same range of temperatures. This result agrees with the reduction of the sensitivity parameter calculated by Jin and Subramanian [31]. Above this temperature all the curves present almost linear behavior with similar slope.

3.3.5. Air as diluent

On the other hand, in the case of H_2 combustion in air with no additional N_2 where the total N_2 concentration varies from 70 to 90 vol%, a flat behavior was predicted, as plotted in Fig. 5(a)–((c). The addition of N_2 to the $H_2 + O_2$ mixture does not modify the gas-like behavior. The cryogenic characteristics of the diluent reduce the mixture critical point below the working conditions. In this way, monotonic and small variations are obtained for the AFT as well as for the LFL values which are lower than the case of CO_2 at the same conditions. This result is explained by the low heat capacity of the N_2 compared to CO_2.

In order to validate the assumption made for the AFT threshold value, Fig. 6 shows the influence of the LFL value at low pressure in the calculation of the AFT threshold value and in the final calculation of LFL in the selected pressure range. From the literature we can accept LFL values from 4.0 to 4.5 vol% for mixtures with air as diluent giving a AFT values between 601 K and 640 K respectively. Differences lower than 6.5% have been found in the prediction of LFL for CO_2 using this AFT range for a 298 K and $H_2/O_2 = 2$ (similar to Fig. 5(a)), therefore the assumption is accepted.

3.4. Speed of sound profiles

A flame can deflagrate if the flame front velocity is lower than speed of sound in the mixture. In addition, an explosion takes place when the flame front is greater than the correspondent speed of sound. In order to observe the behavior of the speed of sound in $H_2 + O_2 + CO_2$ mixtures, two conditions were considered for calculation: the reaction is taking place at high-pressure and the combustion carried out at atmospheric conditions. Both values have been calculated at the final AFT reached in each case. Fig. 7 shows the values of the sound speed calculated using Eq. (19), for a combustion at 288 K and 7 vol% H_2 and $O_2/H_2 = 2$.

$$c = \left(\frac{-V^2 (\partial P / \partial V)_{T,n}}{MW} \right)^{0.5} \tag{19}$$

where MW is the molecular weight of mixture and V is the mixture molar volume.

Fig. 7 shows that speed sound of the mixture increases along with pressure. The speed sound at high pressures (P, AFT) remains always above the line of the speed of sound at atmospheric pressure (1 bar, AFT) for the pressure range investigated. Also, the ratio between these two values varies linearly in this pressure range. For instance, at 150 bar speed of sound increases 10.2% respect to atmospheric conditions. At higher, pressures the variation seems to be lower than the correspondent to linear value (18.4% at 300 bar). These results let us conclude that deflagration, as well as explosion, could be retarded at higher pressures, which might be related to an increase of properties of heat and mass transport in the flame front.

4. Conclusions

The operation under high pressures dealing with flammable mixtures, e.g. for the direct synthesis of H_2O_2, requires the knowledge of the flammability limits. So far, these data is scarce. In this work an estimation method for the lower flammability limit based in the calculation of the adiabatic flame temperature has been proposed. The model has been validated using experimental data for mixtures of $H_2 + O_2$ in CO_2 and N_2, between 0.1 and 300 bar and 288 and 348 K.

The method has been tested using a GC-EoS for the prediction of the thermodynamic properties giving deviations lower than 10% at high pressures in most cases. Similar predictions were carried out using a commercial software, Aspen Plus ONE7 with the property package Soave–Redlich–Kwong EoS with MHV2 mixing rules achieving similar results than with the GC-EoS.

Assuming a constant adiabatic flame temperature of 620 K the mixtures of $H_2 + O_2 + CO_2$ can be predicted with errors between 2.5% and 7.5% from 1 bar to 300 bar. The use of CO_2 as a diluent increases the operational margin from 4.5 mol% H_2 at 1 bar up to ca. 7.0–9.0 mol% H_2 at 200 bar due to the increase in the heat capacity, this increase is especially noticeable near the critical point. On the other hand, the use of nitrogen or air as diluent only increases the margin from 5.2 mol% H_2 at 1 bar up to ca. 6.0 mol% H_2 at 200 bar.

Additionally, we have estimated the speed sound for mixtures of 7 vol% H_2 under explosion conditions, at pressures from 1 bar to 150 bar and the calculated adiabatic flame temperature each case. We have found that that there is an increase of about 10% at higher pressures compared to the speed of sound at atmospheric conditions.

There is a lack of flammability data for mixtures at high pressures. This work initiates the modeling and prediction of the LFL under supercritical conditions, we hope that in the near future there will be more data available and improved models for prediction.

Acknowledgements

The authors express their grateful to Consejo Nacional de Investigaciones Científicas y Técnicas (CONICET) as well as to Universidad Nacional del Sur (UNS) from Argentine for the financial support. The authors also wish to thank the Spanish Ministry of Science and Innovation, Projects Reference: CTQ 2006-0299/PPQ and CTQ2009-14183-C02-01 for financial support, and University of Valladolid for the research mobility fellowship granted. Finally, we wish to thank Dr. Sierra-Pallares for his initial work and scientific advice.

References

[1] R.W. Van Dolah, M.G. Zabetakis, D.S. Burgess, G.S. Scott, Flame propagation, extinguishment and environmental effects on combustion, Fire Technology 1 (1965) 138–145.
[2] L. Catoire, S. Paulmier, V. Naudet, Experimental determination and estimation of closed cup flash points of mixtures of flammable solvents, Process Safety Progress 25 (2006) 33–39.
[3] T.A. Albahri, Flammability characteristics of pure hydrocarbons, Chemical Engineering Science 58 (2003) 3629–3641.
[4] F.Y. Hshieh, Predicting heats of combustion and lower flammability limits of organosilicon compounds, Fire and Materials 23 (1999) 79–89.
[5] W.H. Seaton, Group contribution method for predicting the lower and the upper flammable limits of vapors in air, Journal of Hazardous Materials 27 (1991) 169–185.
[6] M. Vidal, W.J. Rogers, J.C. Hoiste, M.S. Mannan, A review of estimation methods for flash points and flammability limits, Process Safety Progress 23 (2004) 47–55.
[7] M. Vidal, W. Wong, W.J. Rogers, M.S. Mannan, Evaluation of lower flammability limits of fuel-air-diluent mixtures using calculated adiabatic flame temperatures, Journal of Hazardous Materials 130 (2006) 21–27.
[8] F.N. Egolfopoulos, A.T. Holley, C.K. Law, An assessment of the lean flammability limits of CH_4/air and C3H8/air mixtures at engine-like conditions, Proceedings of the Combustion Institute 31 (2007) 3015–3022.
[9] Y.N. Shebeko, W. Fan, I.A. Bolodian, V.Y. Navzenya, An analytical evaluation of flammability limits of gaseous mixtures of combustible-oxidizer-diluent, Fire Safety Journal 37 (2002) 549–568.
[10] G.A. Melhem, A detailed method for estimating mixture flammability limits using chemical equilibrium, Process Safety Progress 16 (1997) 203–218.
[11] J.M. Campos-Martin, G. Blanco-Brieva, J.L.G. Fierro, Hydrogen peroxide synthesis: an outlook beyond the anthraquinone process, Angewandte Chemie International Edition 45 (2006) 6962–6984.
[12] K. Weissermel, H.-J. Arpe, Industrial Organic Chemistry, 4th ed., Wiley-VCH, Weinheim, 2003.
[13] D. Hâncu, E.J. Beckman, Generation of hydrogen peroxide directly from H_2 and O_2 using CO_2 as the solvent, Green Chemistry 3 (2001) 80–86.
[14] J.O. Pande, J. Tonheim, Ammonia plant NII: explosion of hydrogen in a pipeline for CO_2, Process Safety Progress 20 (2001) 37–39.
[15] J.R. Hyde, P. Licence, D. Carter, M. Poliakoff, Continuous catalytic reactions in supercritical fluids, Applied Catalysis A: General 222 (2001) 119–131.
[16] G. Jenzer, M.S. Schneider, R. Wandeler, T. Mallat, A. Baiker, Palladium-catalyzed oxidation of octyl alcohols in "supercritical" carbon dioxide, Journal of Catalysis 199 (2001) 141–148.
[17] T. Moreno, J. García-Serna, M.J. Cocero, Direct synthesis of hydrogen peroxide in methanol and water using scCO_2 and N_2 as diluents, Green Chemistry 12 (2010) 282–289.
[18] T. Moreno, J. García-Serna, P. Plucinski, M.J. Sánchez-Montero, M.J. Cocero, Direct synthesis of H_2O_2 in methanol at low pressures over Pd/C catalyst: semi-continuous process, Applied Catalysis A: General 386 (2010) 28–33.
[19] S. Skjold-Jørgensen, Gas solubility calculations. II. Application of a new group-contribution equation of state, Fluid Phase Equilibria 16 (1984) 317–351.
[20] S. Skjold-Jørgensen, Group contribution equation of state (GC-EOS): a predictive method for phase equilibrium computations over wide ranges of temperature and pressures up to 30 MPa, Industrial and Engineering Chemistry Research 27 (1988) 110–118.
[21] N.F. Carnahan, K.E. Starling, Equation of state for nonattracting rigid spheres, The Journal of Chemical Physics 51 (1969) 635–636.
[22] DIPPR, Physical Properties Database, Project 801, Design Institute for Physical Property Data (2007).
[23] H. Renon, J.M. Prautsniz, Local compositions in thermodynamic excess functions for liquid mixtures, AIChE Journal 14 (1968) 135–144.
[24] S.B. Bottini, T. Fornari, E.A. Brignole, Phase equilibrium modelling of triglycerides with near critical solvents, Fluid Phase Equilibria 158-160 (1999) 211–218.
[25] N.K. Muirbrook, J.M. Prausnitz, Multicomponent vapor–liquid equilibria at high pressures. Part I. Experimental study of the nitrogen–oxygen–carbon dioxide system at 0 °C, AIChE Journal 11 (1965) 1092–1098.
[26] J.O. Spano, C.K. Heck, P.L. Barrick, Liquid–vapor equilibria of the hydrogen–carbon dioxide system, Journal of Chemical Engineering Data 13 (1968) 168–171.
[27] K. Todheide, E.U. Franck, Das Zweiphasengebiet die Kritishe Kurve im System Kohlendiocid-Wasser bis au Drucken von 3500 bar, Zeitschrift Fur Physikalische Chemie 37 (1963) 387–392.
[28] M.G. Zabetakis, Flammability Characteristics of Combustible Gases and Vapors, US Dept. of the Interior Bureau of Mines, 1965.
[29] Y.N. Shebeko, S.G. Tsarichenko, A.Y. Korolchenko, A.V. Trunev, V.Y. Navzenya, S.N. Papkov, A.A. Zaitzev, Burning velocities and flammability limits of gaseous mixtures at elevated temperatures and pressures, Combustion and Flame 102 (1995) 427–437.
[30] V. Schröder, M. Molnarne, Flammability of gas mixtures. Part 1. Fire potential, Journal of Hazardous Materials 121 (2005) 37–44.
[31] H. Jin, B. Subramaniam, Exothermic oxidations in supercritical CO_2: effects of pressure-tunable heat capacity on adiabatic temperature rise and parametric sensitivity, Chemical Engineering Science 58 (2003) 1897–1901.
[32] S. Dahl, M.L. Michelsen, High-pressure vapor–liquid equilibrium with a UNIFAC-based equation of state, AIChE Journal 36 (1990) 1829–1836.
[33] HYSAFE, Hydrogen Ignition, http://www.hysafe.net/download/1042/BRHS_Chap3_hydrogen%20ignition%20version_0_9_0.pdf, 2010.
[34] V. Schröder, B. Emonts, H. Janßen, H.P. Schulze, Explosion limits of hydrogen/oxygen mixtures at initial pressures up to 200 bar, Chemical Engineering and Technology 27 (2004) 847–851.